AFS Transactions 2007 © American Foundry Society, Schaumburg, IL USA

Sponsored Research: Clean Steel Casting Production– Evaluation of Laboratory Castings

S. Kuyucak
CANMET–MTL, Ottawa, Ontario, Canada

ABSTRACT

Wedge-block castings with a 12 × 18 in. cope surface area were poured in AISI 1020 steel, with the standard "gooseneck" gating practice utilizing a pouring cup connected to a straight ceramic tile sprue and the new methoding ideas using a pouring basin with a small dam or a dam and a submerged ladle nozzle extension to minimize air entrainment and reoxidation. The steels were evaluated with respect to casting surface cleanliness.

INTRODUCTION

Water modeling experiments showed 30-60% air entrainment by volume in typical ladle bottom-pouring operations.[1] The air entrainment increases with poured metal head height, it is also well-known that casting surface defects increase similarly.[2] In this regard, the first poured steel castings from a bottom-pouring ladle usually require more rework than those poured later, and lip-poured castings are usually cleaner than those that are bottom-poured. It is envisaged that the turbulence created by the entrained air in the mold cavity is largely responsible for the casting surface defects.

Water modeling experiments showed two viable designs to eliminate entrained air using a pouring basin in the gating system. One employed a small dam near the sprue inlet of the pouring basin, which allowed entrained air to escape to the atmosphere rather than be carried into the sprue; the other had a submerged ladle nozzle extension (shroud) into the pouring basin. The latter design prevented air-entrainment as well as its attendant re-oxidation. The aim of the present study was to determine if eliminating entrained air from the gating system could improve the surface quality of actual castings.

EXPERIMENTAL

Comparative wedge-block castings were made in AISI 1020 steel via a bottom-pouring ladle using a pouring cup or a pouring basin (Fig. 1). Two wedge-blocks were poured from 440 kg heats, the first one utilizing a pouring cup (standard gating); and the second, a pouring basin with a dam, with or without a submerged nozzle extension (alternative gating). The second poured blocks with the alternative gating had a lower metal head in the ladle, but the ladle was raised to clear the pouring basin; thereby, decreasing the difference in pour heights between the two castings. The average pour heights taken from average metal head in the ladle to sprue base (referring to Fig. 1) were:

Standard gating:	45.5"
Alternative gating with or without nozzle extension:	43.0"

The molds were made in silica sand having an AFS grain size number of 55, bonded with 4.5 pct. by sand weight dextrin modified (5pct.) sodium silicate (50 pct. aq.) binder. After removing the gates and risers, the castings were cleaned by sand blasting. Table 1 shows the experimental conditions and the results of cope-surface evaluation. Fig. 2 shows the cope surface photographs of the castings.

The heats F5083 and F5085 were meant to be submerged poured with nozzle extensions. However, the shrouds started to split longitudinally during Pour A and were fully open during Pour B (Fig. 6). It was later found that the manufacturing technique for these components, which consisted of extrusion and joining of four quadrants made of silica into a cylinder, was not suitable. These castings were effectively poured without a nozzle extension.

Manufacturers Standardization Society's Standard Procedure MSS SP-55[3] was used to distinguish which surface irregularities constituted a defect. A square inch grid was prepared on a transparent sheet and laid over the cope surface. Each square on the grid incident on a defect and covered more than 2/3 by that defect was counted as one. If the square was only partially covered (1/3 to 2/3), a half score was given. The total score then was expressed as the "dirt count" of the cope surface. The results are shown in Table 1.

Table 1. Evaluation of Cope-side Defects in Laboratory Castings.

Heat No. / Block ID	Tap temp. / Pour temp. (°C)	Dirt Count	Comments
F5071	1646		Ladle nozzle only. Pour via pouring cup (A) and pouring basin (B).
A	1620	24	Large cope defect at the thin-end.
B	1593	5	Clean except where location for breather holes show in relief.
F5083	1637		Ladle nozzle with extension. Pour via pouring cup (A) and pouring basin (B). Nozzle extension split open longitudinally to four parts during Pour A (Fig.).
A	1591	8	Clean
B	1577	16	Small roughness and ripples
F5085	1645		Ladle nozzle with extension. Pour via pouring cup (A) and pouring basin (B). Nozzle extension split open longitudinally to four parts during Pour A. Pour B was interrupted before the riser started to fill.
A	1603	8	Defects towards thin end and center.
B	1586	24	Very rough, ripples and folds.
F5089	1642		Ladle nozzle only. Pour via pouring cup (A) and pouring basin (B).
A	1603	9	Mostly clean. Open micropores, small ripples.
B	1583	20	Medium rough and ripples.

In all cases except the first one, cope-surface quality of the casting with the alternative gating was less satisfactory. The defects were mostly in the form of ripples, indicating a low temperature in the mold and premature freezing. The successful casting had the highest pour temperature. Effectively, the pouring basin as an intermediate vessel caused an additional heat loss, which needed to be compensated for.

Other than the ripples and cold-shut-like defects caused by the current design with the pouring basin, “Ceroxide”-like defects were often seen (Fig. 3). During shake-out, an adherent sand covered these areas. Upon removing the sand with a knife edge, fine holes could be seen on the steel surface and the facing sand surface had similar features (Fig. 4). It is highly unlikely that these were caused by displaced oxide macro-inclusions.

FLOW SIMULATION

Flow-3D (registered trademark of Flow Science, Inc., Santa Fe, NM) simulations were carried out by the University of Alabama at Birmingham on the proposed and existing pouring systems for the wedge-block castings (Fig. 5). The code also allows the exposed surface area of steel integrated over the pouring time, expressed in (m^2s), to be calculated. These results are shown in Fig. 5b. Typically, the results show that the insertion of a pouring basin into the gating system increases the steel’s exposure to atmosphere.

DISCUSSION

The alternatively gated castings via a pouring basin showed defects related to cold metal. Therefore, an analysis of the heat loss during pouring is first presented to identify the problem. Next, reoxidation effects due to exposed steel surface area are discussed.

Table 2. Calculation of the Temperature Drop in Steel During Pouring

Related material properties and conditions

Material	Density (kg/m^3)	Heat capacity ($J/kg\ m^3$)	Thermal cond. (W/m °C)	Thermal diff. (m^2/s)	Initial temp. (°C)
Sand mold / tile gating [a]	1500[b]	1100	0.65	$0.394\ 10^{-6}$	20
Steel	7000	760			1580[c]

[a]Assume similar properties in sand mold and tile gating. [b]True density of sand is 2600 kg/m^3. [c]Average steel temperature during the pour.

Time to start filling the riser	20 s
Steel contained in the mold cavity and gating (excluding the riser)	170 kg
Moisture content of sodium silicate bonded sand	5%
Thickness of thermal penetration in sand, x(120°C)	7 mm
Latent heat of evaporation of water	2,259,260 J/kg

Temperature loss at different components and the cumulative temperature loss for the two systems considered

Component		Surface area (m^2)		Temp. drop (°C)		Total temp. drop (°C)
		Conducting	Radiating	Conducting	Radiating	
Nozzle extension	pb	0.027	-	1.7	-	
Pouring basin	pb	0.237	0.084	15.0	7.0	
Moisture effect	pb			2.2		
Ladle stream	pc	-	0.009	-	0.8	
Pouring cup	pc	0.036	0.010	2.3	0.8	
Tile gating	pc pb	0.100	-	6.3		
Riser pad and mold cavity	pc pb	0.301	0.180	19.1	14.9	
Moisture effect	pc pb			2.8		
Temperature drop with pouring cup methoding (sum of all pc's)				30.5	16.5	**47.0**
" " pouring basin methoding (sum of all pb's)				47.0	21.9	**68.9**

HEAT LOSS DURING POURING

The heat lost to the tile gating and molding sand is similar to inserting these cold surfaces into the steel melt for the duration of the pouring time. Assuming the average steel temperature to be the constant wall temperature, the temperature profile in the refractory is given by an error function type of solution:

$$\frac{T_{ref} - T_0}{T_W - T_0} = \mathrm{Erfc}\left(\frac{x}{2\sqrt{\alpha\, t}}\right) \quad \text{and} \quad \alpha = \frac{k}{\rho_{ref}\ C_{p,ref}} \qquad \text{Equation 1}$$

where:

T_{ref} temperature in the molding sand / refractory tile at x distance from the wall (°C)
T_0 initial temperature of the molding sand / refractory tile
T_W wall temperature of the molding sand / refractory tile in contact with liquid steel
α thermal diffusivity of molding sand / refractory tile (m^2/s)
k thermal conductivity (W/m °C)
ρ_{ref} apparent density (kg/m^3)
$C_{p,ref}$ heat capacity of the molding sand / refractory tile (J/kg °C)
t time to fill the mold cavity just before the riser starts to fill (s).
Erfc (x) = 1 - Erf (x), is the complementary error function.

Table 2 gives the relevant molding sand / refractory tile and steel properties. The temperature losses in steel during pouring a wedge-block casting are calculated. The following procedure is used and the simplifying assumptions are made:

1. Heat is lost to the wetted refractory surfaces by conduction and from the free surfaces by radiation.

2. The time period considered is the time taken to fill the mold cavity, just before the riser starts to fill. Similarly, the mass of metal considered in the heat balance is that contained by the mold cavity and the gating system, excluding the riser (m_{Fe}). This is so selected because when the riser starts to fill, the metal has already made contact with the cope surface, the mold cavity of interest is full and the freezing may start.

3. First compute the wetted surface area in different parts of the gating system and the mold cavity. For the sides of the pouring basin and the mold cavity, use time-average heights that are wetted. Also, compute the radiating surface areas in the ladle stream, pouring basin, pouring cup, and the mold cavity.

4. Assume an average steel temperature for the duration of the pouring. Based on this temperature, find the temperature profile in the molding sand / tile refractory in time t from Eqn. 1 (T_{ref}). This is shown in Fig. 7, which is also hyperlinked to the Excel spreadsheet where calculations are made. From the specific heat of the media and the wetted area, calculate the amount of heat absorbed by conduction (Q_{con}):

$$Q_{cond} = A_{cond} \int_0^{\infty} \left(T_{ref} - T_0\right) C_{p,ref}\, dx \qquad \text{Equation 2}$$

5. Similarly, calculate the amount of heat lost by radiation in time t (Q_{rad}). Assume emissivity of steel 0.8.

$$Q_{rad} = \Im \varepsilon_{Fe} A_{rad} \sigma \left(\theta_{Fe}^4 - \theta_{sur}^4\right) t \qquad \text{Equation 3}$$

where:

$\Im$	overall interchange factors for radiation (assume 1)
ε_{Fe}	emissivity of steel (0.8)
σ	Stefan-Boltzmann constant (5.67×10^{-8} W/m^2 K^4)
θ	absolute temperature in °K ($\theta = T$+273). Subscript "sur" is for surroundings.

6. Evaporation of moisture from the molding sand also may provide additional cooling in the pouring basin and the mold cavity. This is taken into account by assuming all moisture evaporates in a layer where temperature exceeds 120°C:

$$Q_{moist} = A_{sand}\, x(120°C)\, \rho_{sand}\, g_w L_w \qquad \text{Equation 4}$$

where:

x(120°C)	thickness of thermal penetration layer in sand where temperature reaches 120°C.
g_w	moisture content of sand (wt. pct.)
L_w	latent heat of evaporation of water (J/kg)

7. Once the heat absorbed by all three mechanisms is found, the temperature drop in steel during mold filling is found by:

$$\Delta T = \frac{Q_{cond} + Q_{rad} + Q_{moist}}{m_{Fe} \cdot C_{p,Fe}} \qquad \text{Equation 5}$$

Table 2 shows the calculated temperature drops in pouring wedge-block castings by the standard (pouring cup) and the alternative (pouring basin) methods. The pouring basin method requires an additional 20°C superheat.

The pouring basin was designed to be effective in preventing entrained air from the gating system, but the additional temperature loss it caused was not anticipated in water modeling. For a fair comparison, castings with pouring basin must be poured with an additional superheat. This methoding may yet produce castings of consistently good surface quality if the entrained air is the major contributing factor towards such surface defects. It must be pointed out as well that the casting size was small in relation to the pouring basin used, as seen from the yield (44 pct., Fig. 1). Larger castings will utilize a similarly sized pouring basin, and the temperature loss will be less significant.

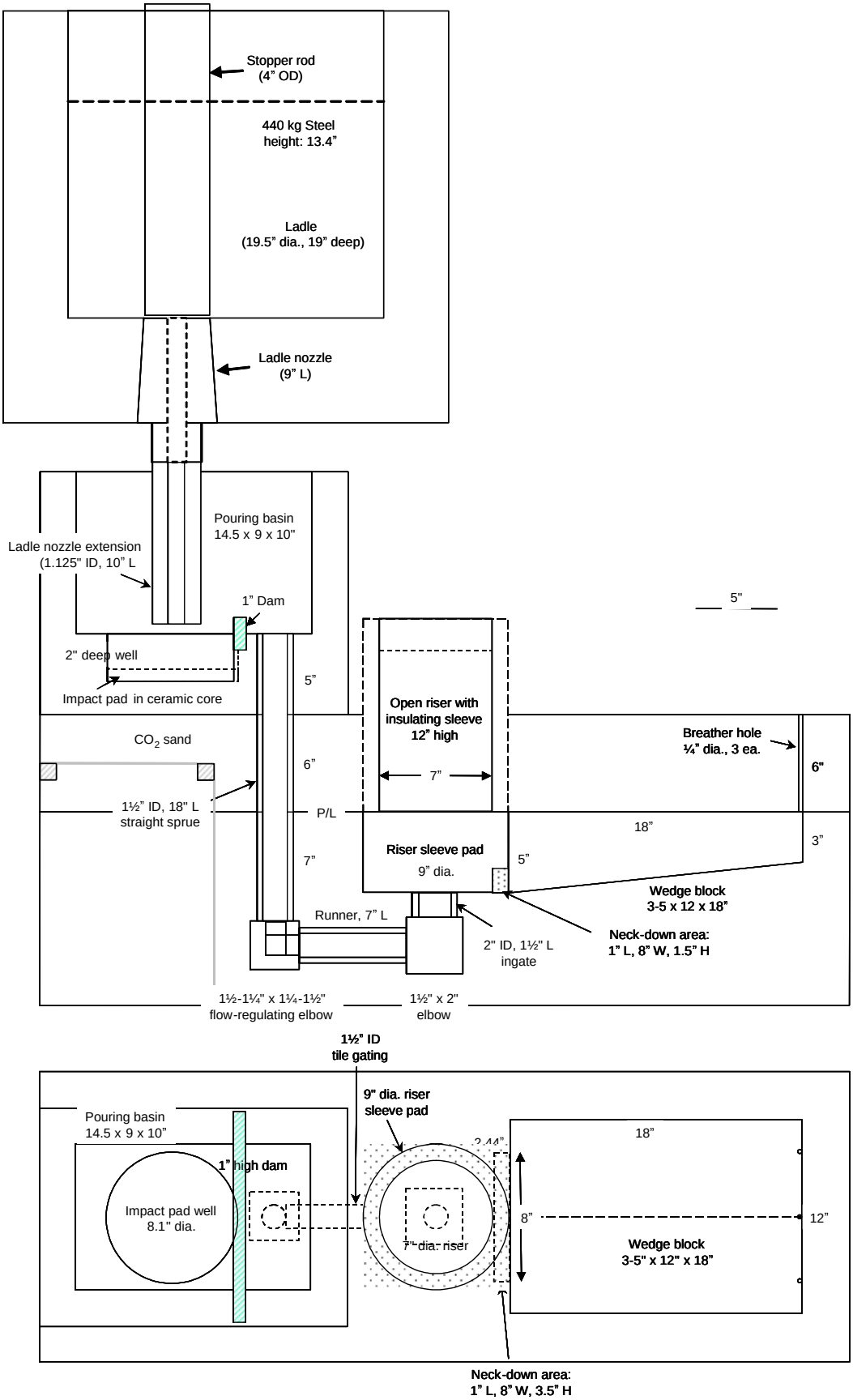

Fig. 1. Methoding of the wedge-block casting with a submerged ladle nozzle extension in pouring basin, side and plan views. Poured weight (with pouring basin): 125 kg, casting weight: 99 kg.

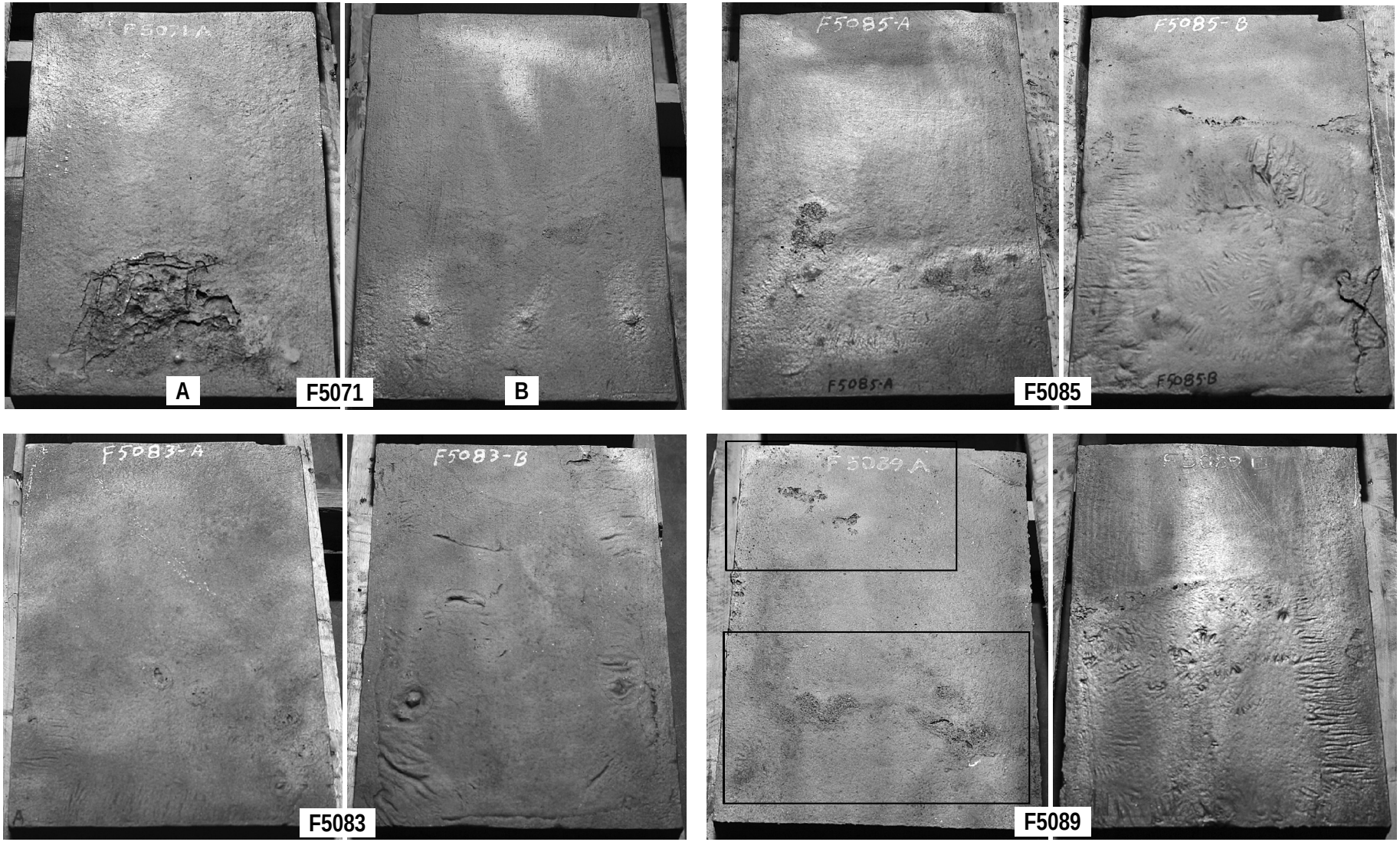

Fig. 2. Wedge-block castings from Heats F5071, F5083, F5085 and F5089. The three spots in relief in both F5071A (towards the front) and B (more visible) are locations for breather holes. The marked areas in F5089A are enlarged in Fig. 3.

Fig. 3. Close-up views from F5089A showing surface defects resembling a "mold blow". These defects are commonly termed "Ceroxide".

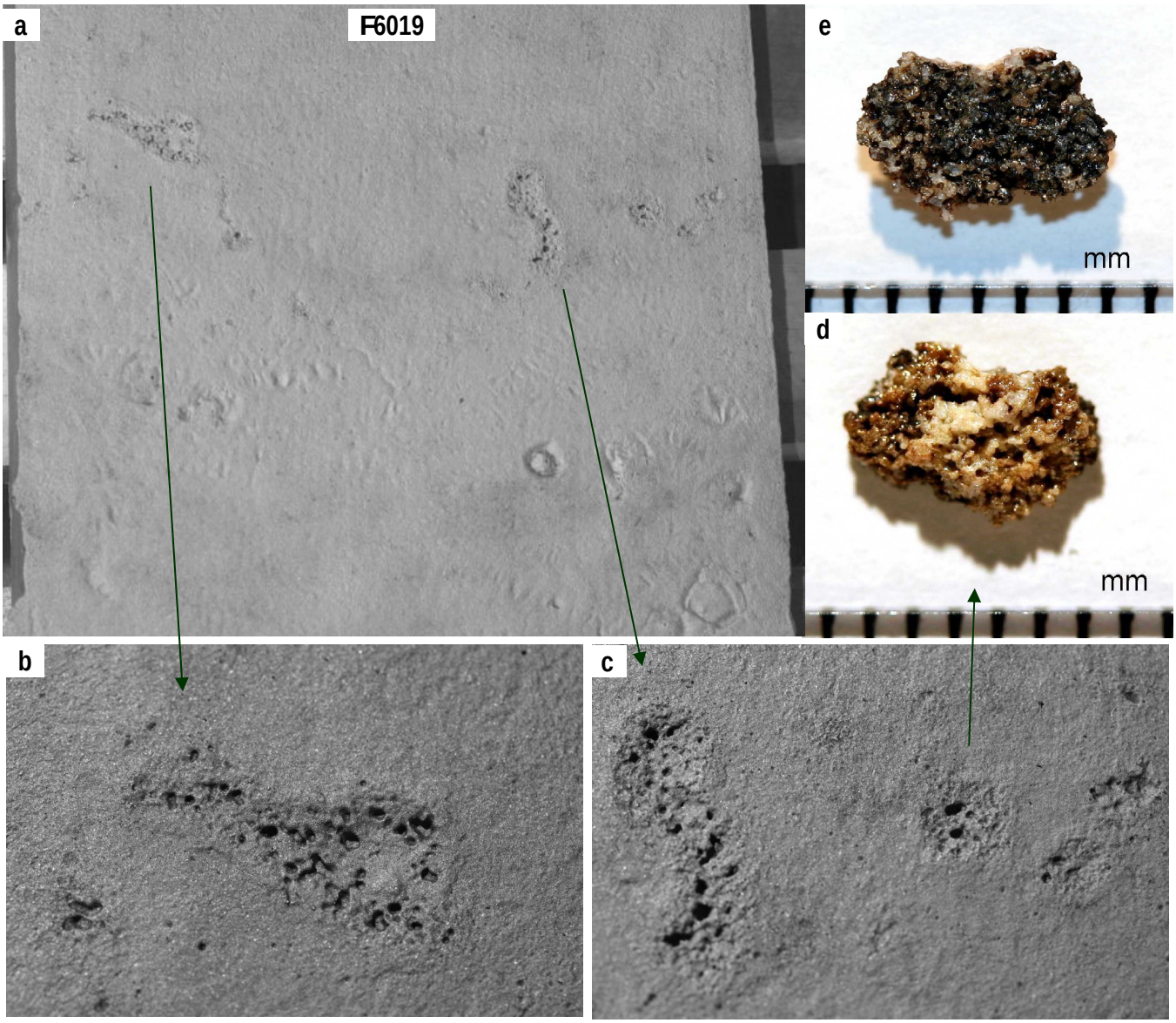

Fig. 4. Wedge-block casting from Heat F6019 (not included in the results), showing more "Ceroxide defects. (a) general view of the cope surface (b) and (c) enlarged views, (d) adherent sand lifted off the defect surface with a knife edge (face attached to steel surface). It has the matching gas holes. (e) the other face of the attached sand showing the beginning of the burnt layer, which extended 2-6 mm into the sand.

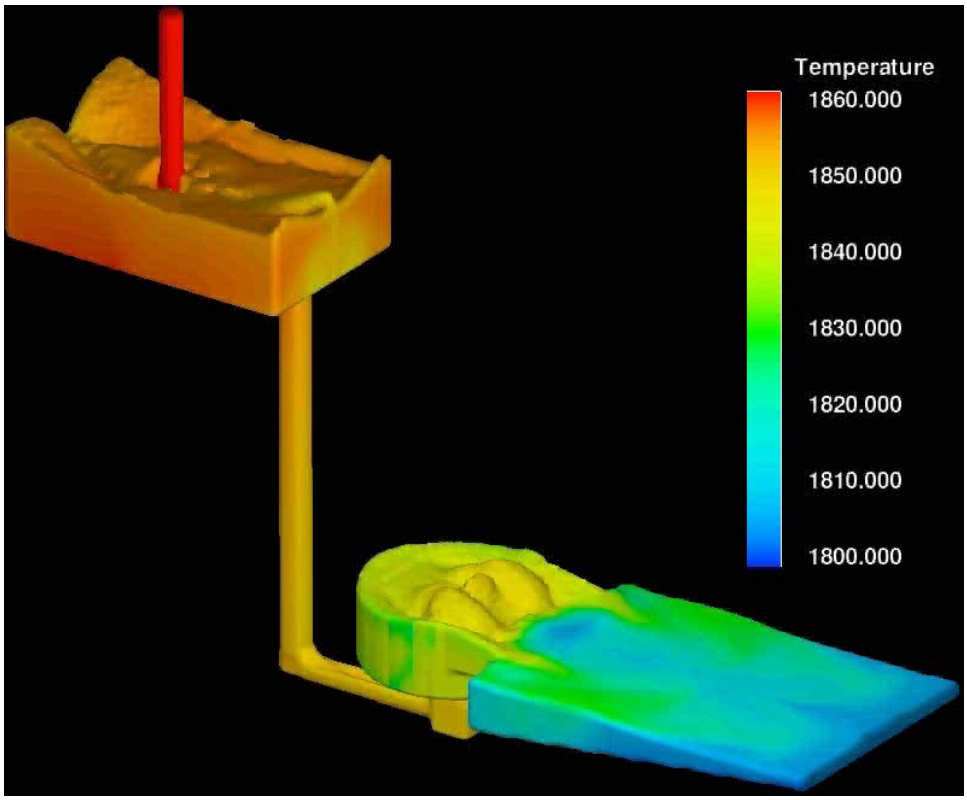

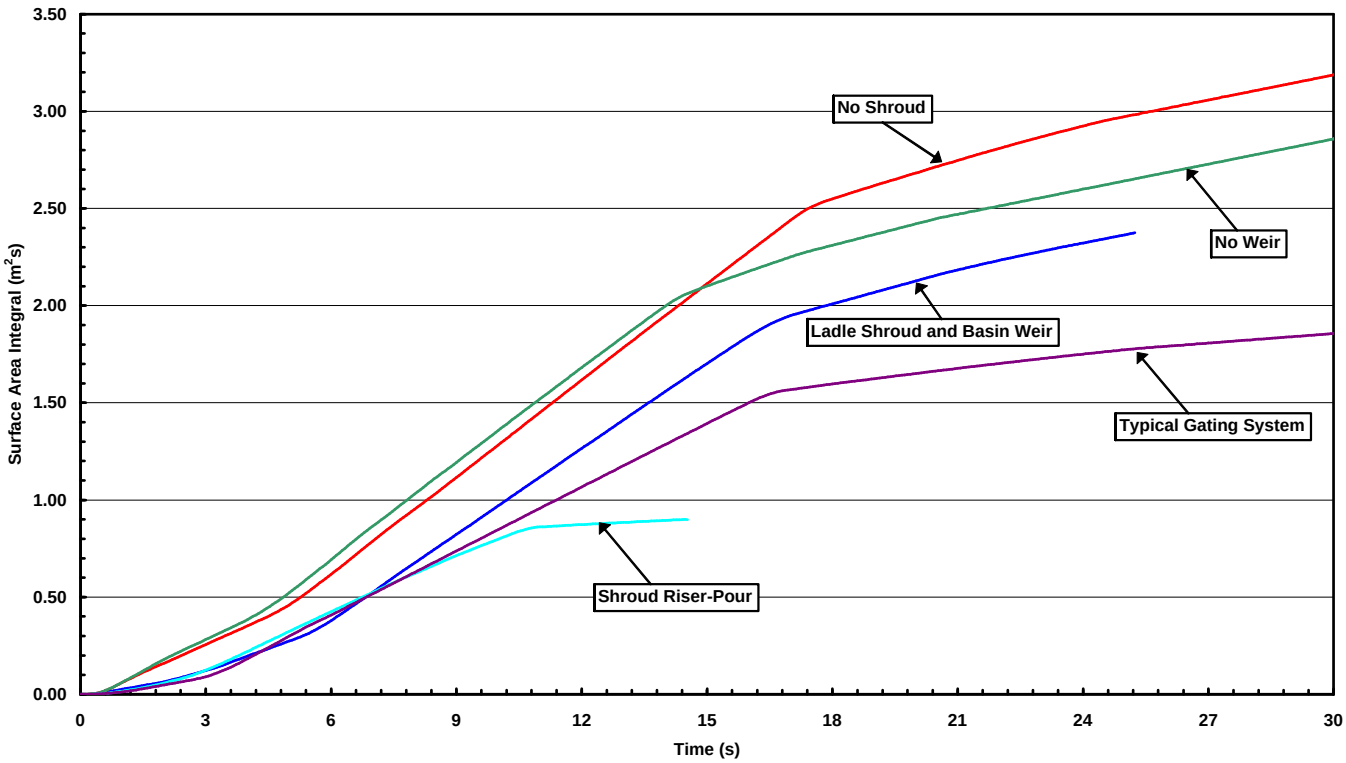

Fig. 5. (a) Flow 3-D simulation of a wedge-block pour utilizing a pouring basin and a submerged ladle nozzle extension (the temperature scale is in °K). (b) Exposed surface area over time integrals for different pours of wedge-blocks.

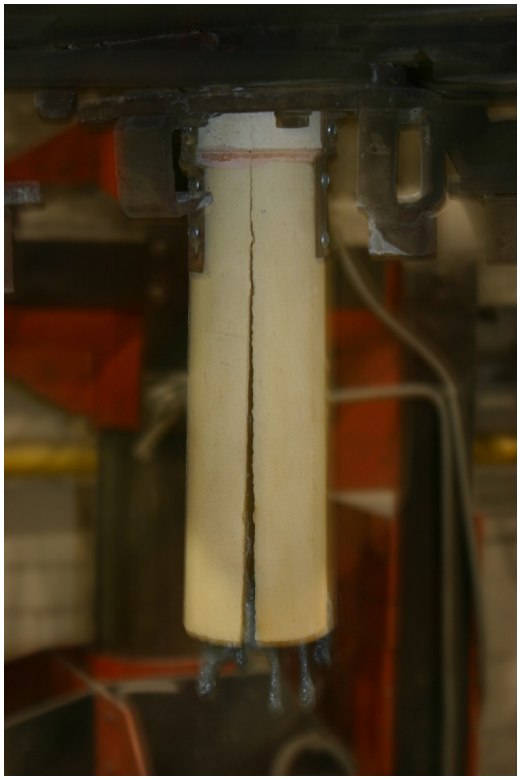

Fig. 6. Nozzle extension that was split open during pouring.

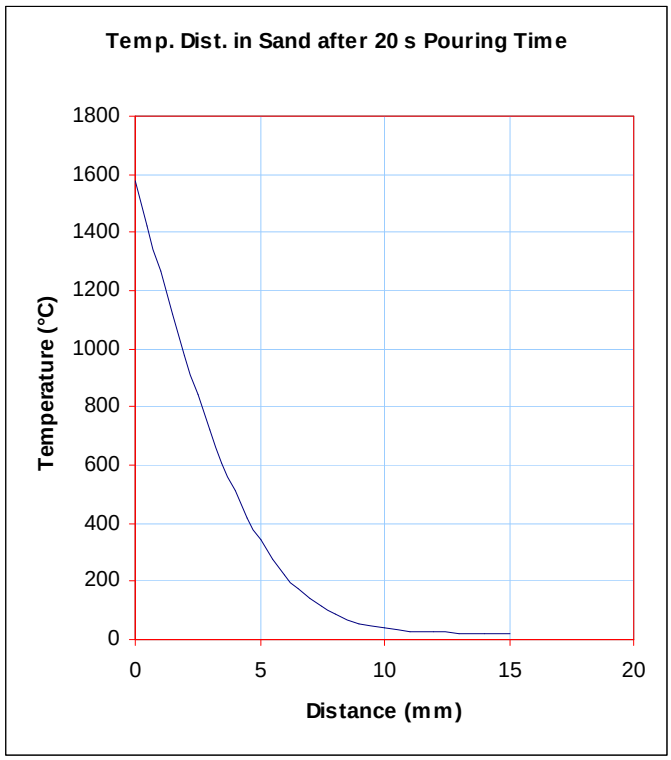

Fig. 7. Temperature distribution in the wetted refractories (molding sand and tile gating) based on the properties and conditions in Table 2.

Temperature drop in steel during pouring is affected mostly by the pouring time. It can be decreased by wider gates. A general rule of thumb is to design a gating system where pouring time is proportional to the square root of the poured weight. If the pouring time is measured in seconds and the weight in lbs, then the recommended constant of proportionality is unity. This relationship establishes a fixed temperature drop for a given type of gating system, and the selected proportionality constant is a compromise between the allowed temperature drop and yield.

RE-OXIDATION DURING POURING

The exposed steel surface area calculations are meaningful only if the degree of reoxidation they lead to is known. Aluminum killed steels are highly reactive towards oxygen; availability of oxygen at the exposed steel surface is typically the rate limiting step. In the following, two approaches have been taken to calculate the degree of reoxidation based on the exposed steel surface area over the pouring time.

Re-Oxidation Through a Boundary Layer

A quasi-steady state rate of reoxidation in killed steels has been suggested by the Japanese workers Sasai and Mizukami:[4]

$$\dot{m}_O = -D_{O2/Air}\left(\frac{C_{O2,0} - C_{O2,\infty}}{\delta_{O2/Air}}\right); \quad C_{O2,0} = 0\,, \quad C_{O2,\infty} = \frac{MW_{O2}\,\rho_{Air}}{MW_{Air}}\,f_{O2,\infty} \qquad \text{Equation 6}$$

where:

$\dot{m}_O$	rate of uptake of oxygen by liquid steel per unit free surface area (kg/m^2 s)
$D_{O2/Air}$	diffusivity of oxygen in air (m^2/s)
$\delta_{O2/Air}$	oxygen boundary layer thickness next to steel surface (m)
$C_{O2,0}$, $C_{O2,\infty}$	oxygen concentration in air next to steel surface and the bulk oxygen conc. in air (kg/m^3)
MW_{O2}, MW_{Air}	molecular weight of oxygen (32 kg/kmol) and air (28.8 kg/kmol), respectively
ρ_{Air}	density of air (kg/m^3)
f_{O2}	volume or mole fraction of oxygen in air

The aluminum activity in de-oxidized steel is such that any oxygen in air next to steel surface is taken up by the steel immediately ($C_{O2,0}$=0) and the supply of oxygen through a boundary layer is the rate-limiting step.

The boundary layer for oxygen depends on the relative movement of air and steel. It varies from 80 mm for still air to as low as 10 mm under highly convective conditions.[5]

Temperature Effects

Air density decreases and oxygen diffusivity increases with temperature. Their effects tend to cancel each other in Eqn. 6:

$$\rho_{Air} = \rho_{Air,20°C}\left(\frac{293}{T}\right) \qquad D_{O2/Air} = D_{O2/Air,20°C}\left(\frac{T}{293}\right)^{1.75} \quad \text{(from Ref. 6)}$$

$$\dot{m}_O = \frac{MW_{O2}\ \rho_{Air,20°C}\ D_{O2/Air,20°C}}{MW_{Air}\ \delta_{O2/Air}}\left(\frac{C_{O2,0} - C_{O2,\infty}}{100}\right)\left(\frac{T}{293}\right)^{0.75} \qquad \text{Equation 7}$$

Oxygen Uptake

The oxygen taken up by the steel in an incremental time Δt is given by:

$$\Delta M_O = \dot{m}_O A_{Fe} \Delta t$$

and the total oxygen uptake during pouring:

$$M_O = \int_0^{t_{pour}} \dot{m}_O A_{Fe}\, dt$$

Substituting for $\dot{m}_O$:

$$M_O = \frac{D_{O2/Air,20°C}\ MW_{O2}\ \rho_{Air,20°C}\ f_{O2,\infty}}{MW_{Air}}\left(\frac{T}{293}\right)^{0.75} \int_0^{t_{pour}} \frac{A_{Fe}}{\delta_{O2/Air}}\, dt$$

$$\text{ppm O} = \frac{D_{O2/Air,20°C}\ MW_{O2}\ \rho_{Air,20°C}}{M_{Fe}\ MW_{Air}}(0.20)(10^6)\left(\frac{T}{293}\right)^{0.75} \int_0^{t_{pour}} \frac{A_{Fe}}{\delta_{O2/Air}}\, dt \qquad \text{Equation 8}$$

where:

M_O	mass of oxygen absorbed by steel (kg)
A_{Fe}	free surface area of steel at a given time during pouring (m^2)
t_{pour}	time to start filling the riser (s)
M_{Fe}	mass of steel poured excluding the riser (kg)

The air temperature next to steel surface can be taken to be the same as that of molten steel (1580°C). But away from the steel surface it will be significantly cooler, as air does not intercept radiation well and convection will bring cooler air from the surroundings continuously. Therefore, an average air temperature for the boundary layer may be taken as 1000°C.

The boundary layer thickness of oxygen depends on the relative movement of steel and air. If an average boundary layer thickness can be assumed, then it can be taken out of the integral. The Flow 3-D simulations basically evaluate the remaining integral $\int_0^{t_{pour}} A_{Fe}\, dt$. The ladle stream is the most turbulent part of the pouring operation and is open to free atmosphere. A very small boundary layer for O_2 (0.01 m) may apply here. But elsewhere, steel flows in confined spaces, surface velocities are smaller and access to fresh air is limited. An overall 0.02 m boundary layer thickness is probably the most representative for pouring. Table 3 gives the evaluated reoxidation for the different cases discussed above and for different pouring systems.

Table 3. Evaluation of Reoxidation in Laboratory Castings.

O-uptake according to Sasai and Mizukami model (Eqn. 8).

Case	Air temp. (°C)	$A_{Fe}\, t_{pour}$[a] (m^2 s)	M_{Fe}[b] (kg)	$\delta_{O2/Air}$ (m)	Re-oxidation (ppm O)
Pouring basin with dam	1580	2.70	170	0.01	29.9
" "	1000	2.70	170	0.01	22.6
" "	1000	2.70	170	0.02	11.3
Submerged shroud to p. basin with dam	1000	2.15	170	0.02	9.0
Standard pour with pouring cup	1000	1.65	170	0.02	6.9

[a]exposed surface area integrated over the pouring time until the riser starts to fill (t_{pour} = 20 s), from Flow 3-D simulations.
[b]steel mass prior to riser starts to fill.

O-uptake according to diffusion / convection model for pouring basin with dam (Eqn. 11).

Case	Air temp. (°C)	$\overline{A}_{Fe}$ (m^2)	M_{Fe} (kg)	t_{pour} (s)	t_r (s)	Re-oxidation (ppm O)
Pure diffusion	1000	0.135	170	20	20	3.8
Diffusion with strong convection	1000	0.135	170	20	1	16.8

Evaluation of Re-oxidation by a Separated Diffusion / Convection Analysis

An alternative approach to reoxidation is given as follows. In the absence of convection, the oxygen supplied to the steel surface is by diffusion only. The oxygen concentration profile in air at a given time *t* is given by:

$$C_{O2,x} = C_{O2,\infty}\,\mathrm{Erf}\left(\frac{x}{\sqrt{4D_{O2/Air}t}}\right) \qquad \text{Equation 9}$$

The oxygen taken up by the steel (kg/m^2) can be found by integrating for the lost oxygen in air starting from the steel surface. This is similar to the analysis for the heat taken up by the sand and tile gating during pouring. Multiplying this result by the *average* exposed surface area will give the total oxygen absorbed. Finally, dividing it by the mass of poured steel will yield the mass fraction of oxygen taken up by the steel:

$$[\text{ppm O}] = \frac{\overline{A}_{Fe}}{M_{Fe}}\frac{MW_{O2}\,\rho_{air}\,f_{O2,\infty}}{MW_{Air}}\left(10^6\right)\int_0^\infty \mathrm{Erfc}\left(\frac{x}{\sqrt{4D_{O2/Air}t_{pour}}}\right)dx \qquad \text{Equation 10}$$

The average exposed surface area $\overline{A}_{Fe}$ is given by dividing the overall exposed surface area by the pouring time.

The effect of convection would be to replace this air with fresh air every so often. Assume replacement occurs every time when time t_r is reached. Accordingly, replace t_{pour} by t_r within the integral, and multiply the result by t_{pour}/t_r for the number of times the replacement occurs during the duration of the pouring:

$$[\text{ppm O}] = \frac{\overline{A}_{Fe}(t_{pour}/t_r)}{M_{Fe}}\left(\frac{32\times 0.20\,\rho_{air}}{28.8}\right)\left(10^6\right)\int_0^\infty \mathrm{Erfc}\left(\frac{x}{\sqrt{4D_{O2/Air}t_r}}\right)dx \qquad \text{Equation 11}$$

When there is no air replacement ($t_r = t_{pour}$), Eqn. 11 reduces to Eqn. 10, the pure diffusion case. By making t_r smaller, oxygen uptake can be increased indefinitely. For a highly convective environment, air replacement may occur every second. Table 3 shows the re-oxidation values for this and the pure diffusion case. Fig. 8 shows the oxygen concentration profiles next to a steel surface for both cases.

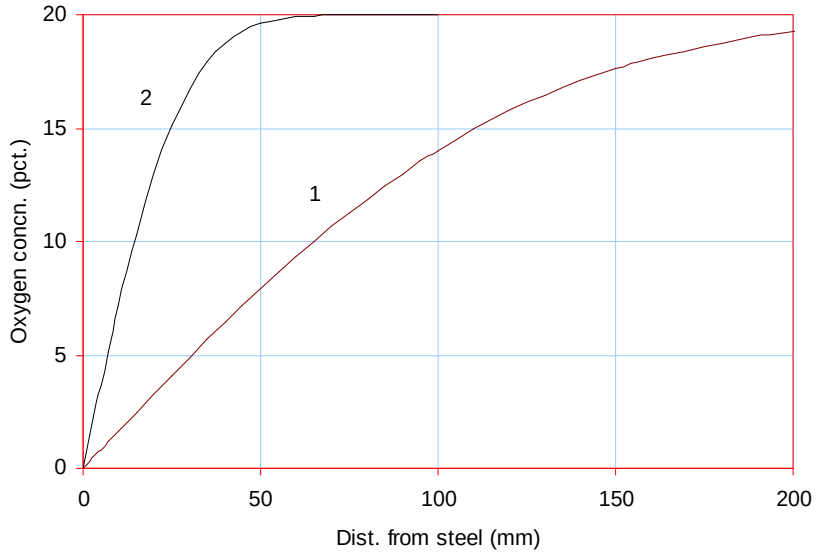

Fig. 8. Oxygen concentration profiles next to a steel free surface during pouring of the wedge-block castings: (1) oxygen supply by diffusion only; (2) convection / diffusion case with a replacement rate of air at 1 per second.

Concluding Remarks for Re-Oxidation

Steel castings typically contain 60-120 ppm O in the form of internal oxide inclusions. In comparison, therefore, reoxidation caused by the exposed surface area of the steel during pouring is not terribly significant. In the worst possible case (pouring basin with dam, no shroud, highly convective environment with the smallest diffusion boundary layer throughout the pour), reoxidation introduces 30 ppm O to the laboratory wedge-block castings. But a more likely value is 10-15 ppm. This is a small rise in total oxygen content to attribute the incidence of casting surface defects to reoxidation. For example, 10-15 ppm O translates to 50-75 ppm by steel volume of oxide defects, [7] or 1.0-1.5 cm^3 of oxide in the present castings. This oxide would be randomly distributed in steel with probably greater incidence on casting surfaces (non-wetting behaviour) and especially the cope surface (flotation), but it is not sufficient to explain the rework needed on most steel castings.

CONCLUSIONS

The new pouring basin designs effectively eliminate or prevent entrained air from the gating system. However, their cooling effect on the present wedge-block castings requires them to be poured at a higher superheat for a fair comparison. For large industrial castings, this will be a lesser problem.

Introduction of a pouring basin also increases the steel's exposed surface area over time during pouring; however, our analysis showed that the accrued reoxidation from this is not significant.

If the premise that turbulence in the mold cavity caused by the entrained air is the major contributing factor to casting surface defects, then the new pouring basins should result in significant improvements. In the next phase of the study, large Industrial castings are planned to be poured using the submerged nozzle entry design at the participating industry sponsor sites.

ACKNOWLEDGEMENTS

The author wishes to thank the US DoE and the Canadian Department of Natural Resources for financial support, industry sponsors (Harrison Steel, Canada Alloy Castings, Maynard Steel, M E Global, Sivyer Steel, Industrial Ceramic Products) for in-kind contributions, AFS Steel Division for steering the project and providing input, Prof. J Griffin and Dr. P Scarber of University of Alabama at Birmingham for Flow 3-D simulations.

REFERENCES

1. Kuyucak S (2006). Sponsored Research: Clean steel casting production - Water modeling studies of bottom-pouring ladle operations. *AFS Trans.*, Paper 06-095.
2. Monroe R W and Blair M (2005). Steel foundry research. WFO Tech. Forum, St. Louis, MO, 19-Apr-05.
3. MSS SP-55 (1996). Quality standard for steel castings for valves, flanges and fittings and other piping components – Visual method for evaluation of surface irregularities. Manufacturers Standardization Society, Vienna, Virginia.
4. Sasai K and Mizukami Y (1996). Effect of stirring on oxidation rate of molten steel. *ISIJ Int.,* 36, (4), pp. 388-3694; in Beckermann, 2006.
5. Beckermann C and Wang L (2006). Prediction of reoxidation inclusion composition in casting of steel. *Met. Trans B,* 37B, (Aug.), pp 571-588.
6. Perry's Chemical Engineers' Handbook (1984). p. 3-285.
7. Kuyucak S (2000). A critical review of gas-related defects in steel castings. *J M Svoboda Int. Conf. on Steel Melting and Refining,* AFS, p. 71.